

## Hepatocyte Nuclear Factors 4a and 1a (Hnf4a and Hnf1a) Regulate Kidney Developmental Expression of Drug-Metabolizing Enzymes and Drug Transporters

Gleb Martovetsky, James B. Tee and Sanjay K. Nigam

Department of Pediatrics, University of California at San Diego, La Jolla, California, United States of America (G. M., S. K. N.)

Department of Biomedical Sciences, University of California at San Diego, La Jolla, California, United States of America (G.M.)

Department of Pediatrics, Dalhousie University and IWK Health Centre, Nova Scotia, Canada (J. B. T.)

Department of Medicine, University of California at San Diego, La Jolla, California, United States of America (S. K. N.)

Department of Cellular and Molecular Medicine, University of California at San Diego, La Jolla, California, United States of America (S. K. N.)

**Running Title:** Hnf4a and Hnf1a regulate drug-handling genes in the kidney

**Corresponding Author:** Sanjay K. Nigam

University of California, San Diego, 9500 Gilman Drive, MC0693, La Jolla, CA 92093

Tel. (858) 822-3482; Fax. (858) 822-3483; E-mail: [snigam@ucsd.edu](mailto:snigam@ucsd.edu)

**Contents:**

29 text pages

1 table

8 figures

48 references

303 words in Abstract

718 words in Introduction

1496 words in Discussion

**Abbreviations:** DME – drug-metabolizing enzyme/transporter; MEFs – mouse embryonic fibroblasts; OATs – organic anion transporters; OCTs – organic cation transporters; PT – proximal tubule; TSS – transcription start site.

## Abstract

The transcriptional regulation of drug-metabolizing enzymes and transporters (here collectively referred to as DMEs) in the developing proximal tubule is not well understood. As in the liver, DME regulation in the PT may be mediated through nuclear receptors which are thought to “sense” deviations from homeostasis by being activated by ligands, some of which are handled by DMEs, including drug transporters. Systems analysis of transcriptomic data during kidney development predicted a set of upstream transcription factors, including Hnf4a and Hnf1a, as well as Nr3c1 (Gr), Nfe2l2 (Nrf2), Ppara, and Tp53. Motif analysis of cis-regulatory further suggested that Hnf4a and Hnf1a are the main transcriptional regulators in the PT. Available expression data from tissue-specific Hnf4a KO tissues revealed that distinct subsets of DMEs were regulated by Hnf4a in a tissue-specific manner. ChIP-seq was performed to characterize the PT-specific binding sites of Hnf4a in rat kidneys at three developmental stages (prenatal, immature, adult), which further supported a major role for Hnf4a in regulating PT gene expression, including DMEs. In ex vivo kidney organ culture, an antagonist of Hnf4a (but not a similar inactive compound) led to predicted changes in DME expression, including among others Fmo1, Cyp2d2, Cyp2d4, Nqo2, as well as organic cation transporters and organic anion transporters Slc22a1(Oct1), Slc22a2 (Oct2), Slc22a6 (Oat1), Slc22a8(Oat3), and Slc47a1(Mate1). Conversely, overexpression of Hnf1a and Hnf4a in primary mouse embryonic fibroblasts (MEFs), sometimes considered a surrogate for mesenchymal stem cells, induced expression of several of these proximal tubule DMEs, as well as epithelial markers and a PT-specific brush border marker Ggt1. These cells had organic anion transporter function. Taken together, the data strongly supports a critical role for HNF4a and Hnf1a in the tissue-specific regulation of drug handling and differentiation toward a PT-like cellular identity. We discuss our

data in the context of the Remote Sensing and Signaling Hypothesis (Ahn and Nigam, 2009; Wu et al., 2011).

## Introduction:

The kidney proximal tubule is involved in reabsorption of water, electrolytes, and organic solutes, tubular secretion and other processes. Some PT transporters play vital roles in the clearance of many substrates, including some metabolic intermediates, xenobiotics and environmental toxins. Importantly, they are also responsible for excretion of many commonly administered pharmaceuticals or their metabolites generated by the cohorts of Phase I and Phase II drug-metabolizing enzymes. Hence, these transporters, which belong to the ABC and SLC gene families, are commonly grouped as Phase III drug transporters.

The Phase I and II processes of drug metabolism, which result in chemical modification and conjugation of drugs, respectively, have been largely studied in hepatocytes. However, a significant number of genes associated with Phase I and II reactions are expressed in the kidney, some of which have been shown to serve important functional roles (Lash et al., 2008; Lohr et al., 1998). While much remains to be understood regarding the contribution of genes involved in proximal tubule cell systemic and Phase I, Phase II, and Phase III metabolism, even less is known about the transcriptional regulation of these genes.

Little is understood about how DME expression is coordinated in the developing and postnatal PT, in part because many knockout models aimed at studying the kidney experience developmental defects prior to PT formation. The best characterized transcriptional regulator of physiologically relevant transporters in the PT in vivo is Hepatocyte Nuclear Factor 1 alpha (Hnf1a). While still able to form upon complete Hnf1a ablation, the proximal tubule exhibits several transport deficiencies, similar to the characteristics of Fanconi syndrome in humans

(Pontoglio et al., 1996). It is possible that expression of Phase I and Phase II genes was altered as well, but this remains to be studied in detail.

While regulation of the DME repertoire in the PT remains to be explored, we have previously performed a focused study on the regulation of the organic cation transporter Slc22a1 (Oct1), and organic anion transporters Slc22a6 (Oat1) and Slc22a8 (Oat3), in cultured kidney tissues. These transporters are highly enriched in the proximal tubule, where they mediate the rate-limiting uptake step of many drugs and toxins (Burckhardt and Burckhardt, 2011; Giacomini et al., 2010; Nigam and Bhatnagar, 2013; Nigam et al., 2007). They have also been hypothesized to function as part of a larger “remote sensing and signaling” system in whole organism homeostasis (Ahn and Nigam, 2009; Wu et al., 2011). We found multiple lines of evidence suggesting that the nuclear receptor Hepatocyte Nuclear Factor 4a (Hnf4a) may be involved in their regulation, which was further supported by detection of Hnf4a binding in rat kidneys at all three promoters in vivo (Gallegos et al., 2012).

Nevertheless, more direct and functional evidence is lacking. In this study, we sought to identify transcriptional regulators involved in the initiation and maturation of DME expression at distinct stages of prenatal and postnatal PT development. Systems analysis of previously published microarray expression data suggested a large role for Hnf4a in regulating Phase I and Phase II drug-metabolizing enzymes and Phase III drug transporters. Based on the important role of genomic enhancer elements in establishing cell-specific expression (Heinz et al., 2010; Shen et al., 2012; Visel et al., 2009), which is in part defined by expression of specific Phase I, II and III genes in the PT, we set out to characterize the genome-wide localization of p300 in adult rat kidney cortex, where proximal tubules make up the dominant cell fraction. Motif analysis of

enhancer elements identified Hnf4a and Hnf1a as the major “lineage-determining” factors of the PT.

To gain more insight into Hnf4a-dependent transcriptional regulation during development, we analyzed publically-available microarray expression data from five different WT and Hnf4a KO tissues: embryonic liver, embryonic and adult colon, adult small intestine and adult B-islet cells. All tissues exhibited some degree of differential DME expression as a result of Hnf4a ablation, with liver exhibiting the most severe effects. Hence, to better understand PT-specific role of Hnf4a, we used ChIP-seq to determine its binding profile in rat PTs at three progressive stages of PT development: E20, 2 weeks and 8 weeks. Hnf4a binding was found to be correlated to levels of DME expression in PTs. A small molecule antagonist was used to show that Hnf4a regulates key representative Phase I, Phase II and Phase III genes in ex vivo rat kidney cultures. Finally, lentiviral-mediated transduction of Hnf1a and Hnf4a into mouse embryonic fibroblasts (MEFS) induced the expression of proximal tubule Phase I, II and III genes. Together, these findings reveal the pivotal role of Hnf4a and Hnf1a in coordinating DME expression in the developing and postnatal proximal tubule.

## Materials and Methods:

### Microarray Expression Analysis

Seven separate analyses were performed: a comparison of embryonic and adult mouse proximal tubule cell expression, a time series of expression in whole rat kidneys, and five comparisons of wildtype and Hnf4a knockout mouse tissues. To compare expression in prenatal and postnatal proximal tubules, we analyzed publicly available mRNA expression data from proximal tubules isolated from E15.5 (GSM144594-144595, GSM152247-152249) (Brunskill et al., 2008) and adult mouse kidneys (GSM256959-256961 (Wright et al., 2008), GSM490067-490069). Time series data was obtained from a previously published study (Tsigelny et al., 2008), and restricted to genes determined to be enriched in the proximal tubule (Brunskill et al., 2008). To investigate the tissue-specific changes in DME expression upon Hnf4a deletion, the following datasets were analyzed: GSE3126 (E18.5 liver (Battle et al., 2006)), GSE3116 (E18.5 colon (Garrison et al., 2006)), GSE11759 (adult colon (Darsigny et al., 2009)), GSE3124 (adult small intestine), and E-MEXP-1729 (adult isolated B-islet cells (Boj et al., 2010)). Microarrays for each of the seven analyses were prepared separately with Genespring 12.5 software using the RMA algorithm. Probes were discarded within each analysis group unless they had present flags in more than half of the samples in at least one sample group (E15.5/Adult PT, Hnf4a WT/KO tissue) or time-point (E13-E21, P0, 1WK, 4WK, Adult), as determined by the MAS5 algorithm. For the whole rat kidney data, sex chromosome-linked genes were excluded as well. Many genes are represented by more than one probeset; Figure 1A, 2A, and 4A depict differential probeset signal intensities, while Figure 1B, 1C and 4B consider the average of corresponding probe intensities for each gene. In the comparison of expression in pre and postnatal proximal tubules,



differential expression was defined as having more than a 2-fold change (FC) with  $p < 0.05$  with the Benjamini Hochberg correction. For pairwise comparisons of WT and Hnf4a  $-/-$  tissue, it was important to be as inclusive as possible in order to consider changes from tissues with weaker phenotypes. Thus, the cutoff was lowered to  $FC > 1.3$  with  $p < 0.05$ , and no multiple testing correction was applied to increase the solution space. It should be noted that even though all of the five experiments were conducted in mice, two different array platforms were used: Affymetrix mouse 430\_2 (45,101 probe sets) and mouse 430A (22,690 probe sets). Overall, the 430\_2 array is more thorough and has a higher probe/gene ratio. Embryonic colon and small intestine were analyzed using the 430A array, therefore, the differential expression may be underrepresented relative to the other three tissues. To define proximal tubule-enriched gene expression in the kidney during development, a conversion algorithm integrated within GX 12.5 was used to translate probes determined to be enriched in the early mouse proximal-tubule to the rat 230 2.0 platform. For network analysis, probe IDs were imported into the Ingenuity Pathway Analysis software suite (IPA). Core analysis was conducted using the default settings. Upstream regulators were selected based on molecule type and prediction z-score above 2.0.

### **Chromatin Immunoprecipitation**

ChIP was performed as previously described (Gallegos et al., 2012) with some modifications. Isolating proximal tubules from adult kidneys requires enzymatic and mechanical manipulation – processes which can alter the native state of proximal tubule cells before the ChIP part of the technique is performed. To preserve the endogenous chromatin landscape of cells, freshly-isolated kidneys from unsexed E20, P13 or male adult Sprague Dawley rats – corresponding to the three states of DME regulation in the proximal tubule identified by the

developmental time series analysis in the context of proximal-tubule genes – were collected as previously described (Tsigelny et al., 2008) and immediately frozen in liquid nitrogen. To isolate kidney cortex, a frozen whole adult kidney was kept frozen within a ceramic mortar surrounded by dry ice while the outer ~1mm was shaved off with a razor. Whole kidneys or isolated cortex were thawed and minced in 1% formaldehyde in PBS on ice, followed by rotation for 15 minutes at room temperature. Fixation was quenched with glycine for 5 minutes. Fixed samples were then homogenized with a tissue grinder, washed twice with cold 0.5% IGEPAL CA-630 in PBS, and further disrupted in the same buffer using a type A glass dounce homogenizer. Nuclei were pelleted and sonicated on ice (three 5 minute cycles of 30 seconds on/30 seconds off) in ChIP buffer using a Cole Palmer handheld sonicator. To quantify the chromatin and for use as control samples, “input” samples were prepared from the chromatin by treatment with first RNase and then Proteinase K, further de-crosslinking overnight at 65C, phenol extraction and ethanol precipitation. Concentrations were determined using a NanoDrop. ChIP for Hnf4a was performed in duplicate using 20ug of chromatin from E20, P13 and adult whole kidneys and 4ug antibody (Santa Cruz, sc-8987); for p300, 2ug of chromatin from adult cortex and 10ug antibody (Santa Cruz, sc-585) was used. A mix of pre-blocked protein A/G beads was used to recover antibody-bound complexes, which were subsequently washed and eluted with SDS-containing buffer. The DNA was purified from the enriched samples as described above for the input samples.

### **Massively Parallel Sequencing and Analysis**

Libraries were prepared using the Illumina ChIP-seq DNA Sample Prep Kit, using either the pooled duplicates for the ChIP samples or 50ng for the inputs. Amplified DNA fragments

within 200-400bp long were sequenced using the HiSeq 2000 instrument and aligned to the rn4 genome by BIOGEM (Genomics Data Analysis Services, UCSD) according to the standard Illumina pipeline. All further analysis was performed using the HOMERv3.13 software package (Heinz et al., 2010). Clonal reads were removed, and default settings designed for ChIP-seq analysis were used to define and annotate peaks, and calculate measures for quality control. The raw reads and peak files have been deposited in NCBI's Gene Expression Omnibus database under the GEO series accession number GSE50815

(<http://www.ncbi.nlm.nih.gov/geo/query/acc.cgi?acc=GSE50815>).

\*DELETE IN PROOFS - Link for reviewers:

<http://www.ncbi.nlm.nih.gov/geo/query/acc.cgi?token=ubqlgogebrcznkb&acc=GSE50815>

HOMER software was also used to generate files for peak visualization in the UCSC Genome Browser, as well as to calculate overlapping and differentially bound peaks between the 4 samples. Motif enrichment within promoter-distal peaks was calculated with default settings in HOMER, except the number of background sequences was increased to be over five times higher than the number of peaks.

## **Organ and Cell Culture**

Kidneys were dissected from E13.5 Sprague Dawley rat embryos and cultured on Transwell filters in DMEM/F-12 media supplemented with 10% FBS and 1% Pen/Strep, as previously described (Sweet et al., 2006). Media was changed every three days. After 6 days, cultures were treated in triplicate with either 1:1000 DMSO, 2.5uM and 5uM Hnf4a antagonist BI6015 [2-Methyl-1-(2-methyl-5-nitrophenylsulfonyl)-1H-benzo[d]imidazole (Kiselyuk et al.,

2012)], or 10uM of the analogous inactive compound BI6018 for 12 hours (both kindly provided by Dr. Fred Levine, Sanford Burnham Research Institute). Samples were then stored in RNAlater (Ambion) until further processing for RT-qPCR.

MEFs were prepared from E16.5 mouse embryos using a modified version of a previously described method (Sekiya and Suzuki, 2011). Embryonic tissue (excluding CNS and visceral organs) was minced and digested in 0.25% Trypsin in DMEM containing DNase I at 37C in a shaker, periodically being agitated with a pipettor. The resulting suspension was gravity pelleted for 2 minutes to allow large undigested pieces of tissue to settle. The supernatant was collected, pelleted, and resuspended in L-15 media with 1% Pen/Strep, filtered through several layers of sterile gauze, and then twice through 40 micron cell strainer. Resulting cells were again pelleted and frozen (in 45% DMEM, 45% FBS, 10% DMSO) for future use. All animal procedures were approved by IACUC.

### **Immunofluorescence**

Kidney organ cultures were fixed in 4% formaldehyde in PBS at 4C overnight, and then kept in PBS at 4C until staining. The filter membrane was cut out from the Transwell, residual glycine was blocked with 50mM Glycine in PBS, followed by blocking in PBS with 10% BSA, 0.1% Tween 20 and 0.05% Triton-X 100 for one hour at room temperature. Samples were then incubated with mouse E-cadherin antibody (Zymed) in IHC buffer (2% BSA, 0.1% Tween 20, 0.05% Triton-X 100) overnight at 4C. After three-one hour washes in IHC buffer at room temperature, samples were incubated with anti-mouse Cy5 (Jackson ImmunoResearch), rhodamine-conjugated Dolichos Biflorus (Vector Labs) and DAPI at 4C overnight. After three-

one hour washes with 0.1% Tween 20 in PBS, samples were mounted with Fluormount, sealed, and imaged using the Olympus FluoView FV1000 confocal microscope.

### **Lentiviral Transduction**

Lentiviral plasmids pWPI-mHnf4a and pWPI-mHnf1a (Huang et al., 2011) were kindly provided by Dr. Lijian Hui, Shanghai Institute of Biochemistry and Cell Biology. To produce lentiviral vector, Fugene HD (Promega) was used to co-transfect HEK293T cells at ~50% confluency with pWPI-Hnf4a or pWPI-Hnf1a, psPAX2 (Addgene) and pCMV-VSVG(Miyoshi et al., 1998) in DMEM/F-12 media with 10%FBS and 1% Pen/Strep. After 24hr, media was replaced, then collected at 48 and 72 hours, and kept at -80C until use. MEFs were plated the day before infection, and infected overnight at ~40% confluency with media mixed 1:1 with viral supernatant, or 2:1:1 when infecting with both Hnf1a and Hnf4a, in the presence of 8ug/mL Polybrene (Sigma-Aldrich). On the next day, MEF media was replaced with DMEM/F-12 containing 1% FBS, 1% Pen/Strep, 1X Insulin/Transferrin/Selenium (Invitrogen), 20ng/mL EGF (R&D Systems), 4ng/mL Triiodothyronine (Sigma-Aldrich), 20ng/mL Dexamethasone (Sigma-Aldrich), 10ng/mL Cholera Toxin (Sigma-Aldrich) for both infected and uninfected cells. For all assays, cells were sampled 3 days after switching the media. Because pWPI includes EGFP downstream of the insert, we used FACS to quantify transduction efficiency. Of the live cells, based on forward and side scatter, ~70-80% were positive for EGFP.

### **Real Time qPCR**

RNA was extracted from cultured embryonic kidneys and MEF cultures using the RNeasy Micro Kit (Ambion), and cDNA was made using SuperScript III First Strand cDNA

Synthesis Kit (Thermo Scientific). Real Time PCR was carried out using a 3-step cycle on the 7900HT Fast Real-Time PCR instrument (Applied Biosystems) with Power SYBR Green Master Mix (Applied Biosystems). Melt curves were examined to confirm primer specificity. The list of primer sequences is included in Supplemental Table 1.

### **6-Carboxyfluorescein Uptake Assay**

Uninfected and transduced MEFs were washed with PBS, and incubated in either PBS, PBS with 10uM 6-CF, or PBS with 10uM 6-CF and 1mM Probenecid in triplicate at room temperature for 10 minutes. Cells were then washed three times with cold PBS, and levels of fluorescence were measured using a model 1420 Multilabel Counter (PerkinElmer). Assays were performed as previously described (Nagle et al., 2011; Sweet et al., 2006).

## Results:

### **Curating an extensive list of Phase I, II, and III genes**

To begin our analysis of DME transcriptional regulation in the proximal tubule, it was first necessary to define a list of genes potentially involved in Phase I, II or III drug-metabolism. We employed several different sources for the purpose of curating such a list (Table 1). For so-called Phase I and II enzymes, we first included all of the gene families containing classically accepted DMEs (Aldh, Cyp, Gsta, Sult, Ugt, etc.) (Aleksunes and Klaassen, 2012). In order to work with the broadest possible list (that may also be relevant to the handling of toxins and endogenous metabolites), additional enzymes were then added either based on their ability to catalyze the same class of reactions that are carried out by known DMEs, or previous studies (Lee et al., 2011; van den Bosch et al., 2007) suggesting the gene's involvement in Phase I or II reactions. Paralogs and orthologs of known DMEs were included as well. For phase III transporters, we included all members of Abc and Slc transporter subfamilies that include known drug transporters, as classified by the UCSF-FDA TransPortal (Morrissey et al., 2012) (Abcb, Abcc, Abcg, Slc10, Slc21, Slc22, Slc47, Slc51). Some of these transporter family members are associated with metabolite rather than drug handling. However, transporters can typically transport a range of chemical moieties, metabolite handling is commonly reported for classical drug transporters, and many metabolic transporters can bind or transport drugs. Examples of drugs and endogenous substrates are included in Supplemental Table 2. The list of "clinically-relevant" DMEs continues to evolve, particularly for non-hepatic tissues; so, at this first stage, we aimed for inclusivity. However, data was collected from multiple species; some gene IDs chosen based on human data may or may not exist as identically-named homologs in rodents,

and vice versa. Others might exist only in rat or mouse, but not both. The resulting list is summarized in Table 1.

### **Analysis of changes in DME expression during pre and postnatal kidney development identifies a set of potential transcriptional regulators**

We sought to determine how the DMEs were transcriptionally regulated throughout pre and postnatal renal development. Of 455 DMEs (201 Phase I, 183 Phase II, 71 Phase III) annotated on the Mouse 430 2.0 microarray platform, 297 were expressed in either embryonic or adult proximal tubules, of which 159 were significantly changing ( $p < 0.05$ ) at least 2-fold (Fig. 1A, Supplemental Table 3). Of those 159, 66 belonged to Phase I, 71 belonged to Phase II, and 22 belonged to Phase III. Interestingly, 37 of the 159 changing DMEs were found to be downregulated in adult proximal tubules compared to embryonic kidney, indicating selective regulation of DMEs opposed to a general increase in expression of “terminal differentiation” genes, as is sometimes assumed to be the case.

The list of 159 significantly changing genes, along with corresponding log ratios, was then analyzed using the Ingenuity Pathway Analysis software suite (IPA). Upon analyzing changes of DME expression in proximal tubules from E15.5 to adulthood, 7 upstream transcriptional regulators were predicted to be activated: Hnf4a, Nr3c1 (Gr), Nfe2l2 (Nrf2), Ppara, Hnf1a, Tp53 and Nr1i3 (Car). However, the IPA knowledge base compiles information from multiple tissues, species and experimental models, which can introduce error when looking for the most likely regulators of gene expression in particular tissue. To help resolve this, we examined the expression of the predicted regulators in E15.5 and adult proximal tubules, shown in Figure 1B. Multiple studies have reported expression of Hnf1a in the proximal tubule, and deletion of Hnf1a



leads to broad defects in proximal tubule transport function in mature animals (Pontoglio et al., 1996). Figure 1C displays these transcription factors in the predicted regulatory network, with their corresponding predicted targets. While the Car nuclear receptor is heavily associated with regulating drug metabolism in the liver, it was omitted from the network because it is not significantly expressed in the kidney. The remaining predicted transcriptional regulators – Tp53, Hnf4a, Nfe2l2, Ppar alpha, Hnf1a, and Gr – are highly expressed in prenatal and adult proximal tubules. If one further examines the level of connectivity, it is noteworthy that Gr, which is thought to regulate proximal tubule maturation in vivo, and Hnf4a, were both connected to 33 predicted targets; this was followed by a decline in connectivity to 26, 22, 18 and 17 for Nfe2l2, Ppara, Hnf1a and Tp53, respectively.

### **Analysis of the proximal tubule transcriptome during developmental time points reveals a dominant contribution of DMEs**

Nevertheless, sampling proximal tubule expression at two extremes along the developmental spectrum does not provide sufficient resolution to determine the dynamics of this transition. While proximal tubule expression profiles have not been collected from other time points, a thorough time series of genome-wide expression data has previously been collected from whole rat kidneys at various stages of development (Tsigelny et al., 2008). Although physiological studies clearly indicate that the proximal tubule is an important site of drug metabolism and transport, due to the many cell types that make up the kidney, it is difficult to attribute the expression profile of widely-expressed genes in the whole developing and adult organ to any single cell type. Therefore, we restricted our analysis to proximal tubule-enriched genes, as previously defined (Brunskill et al., 2008). When focusing on DMEs that are enriched in the proximal tubule in the kidney, it became apparent that they are a major contribution to proximal

tubule cell gene expression. Even though those DMEs in our classification account for less than 3% of all protein-coding genes, they make up approximately 12% of the total PT-enriched kidney transcriptome (Fig. 2). Furthermore, the dynamics of DME regulation were revealed. Initial induction of DME expression can be seen in late embryonic stages, followed by a surge shortly after birth, and continues to increase into puberty. While it is conceivable that a fraction of the observed increases in transcription might be attributed to a rising fraction of proximal tubule cells, it is important to emphasize that many accepted proximal tubule markers do not change. This suggests regulatory mechanisms independent of cell number. Based on the expression profile of PT-enriched genes, we concluded that three distinct stages minimally describe the transitions in proximal tubule transcription: late embryonic development, postnatal maturation, and adulthood. In mature proximal tubule cells, DMEs are some of the highest expressed genes. This suggests that transcriptional regulatory mechanisms involved in proximal tubule maturation likely include those playing a key role in the regulation of DMEs.

### **Motif analysis of Ep300-bound cis-regulatory elements in the developing kidney suggests Hnf4a and Hnf1a as key regulators**

While we had already established a list of top candidate transcriptional regulators of DMEs, we sought to isolate the dominant contributor(s). Recent data from the ENCODE project and other published work indicates that cis-regulatory enhancer elements are key determinants of cell-specific expression, and they are enriched in binding motifs and binding events of transcription factors responsible for lineage determination (Dunham et al., 2012; Heintzman et al., 2009; Heinz et al., 2010; Shen et al., 2012). Thus, we set out to characterize the co-localization of a known enhancer marker, Ep300, in adult rat proximal tubules using ChIP-sequencing. We obtained high quality data in terms of signal-to-noise and number of peaks; the

ChIP-seq yielded 11,726,046 unique mappable positions for p300, and 7,785,098 for the control input sample in the rn4 genome build. 18% of the mapped reads were contained within highly enriched regions, resulting in 42,537 peaks (Fig. 5A). Of those 20,590 were located in intergenic regions, 14,252 in introns, 906 in exons, and 7,439 in promoters [-1000 to +100bp relative to transcription start site (TSS)]. Based on the literature (Heintzman et al., 2007), this distribution is consistent with expectations of specific p300 marks. Screenshots of representative peaks are displayed in Figure 3A.

Ep300 cannot directly bind DNA; rather, it enhances transcription by interacting with DNA-bound transcription factors. Thus, the detected binding sites are contingent on the presence of recruiting transcription factors. We used the HOMER software, which has previously been effectively used to identify functional motifs (Heinz et al., 2010), to perform motif analysis on 34,034 “distal” enhancers, defined by peaks located more than 1Kb upstream and 500bp downstream of annotated TSSs. Consistent with our earlier pathway analysis, the HOMER software determined that the highest enriched de novo motif best matched the known binding motif for Hnf4a (Fig. 3B). The second most enriched motif was the target sequence for Ctcf, an insulator protein that helps establish chromatin architecture. This finding of Ctcf agrees with previous studies, which found CTCF enrichment at enhancers (Shen et al., 2012) and DNaseI hypersensitive sites (Xi et al., 2007). Interestingly, the third most enriched motif matched the known Hnf1a motif, a known regulator of proximal tubule cell identity. As already mentioned, the contribution of Hnf1a to mature proximal tubule function has been previously examined in a mouse knockout model, but the role of Hnf4a and Hnf1a in the developing proximal tubule, especially with respect to DME regulation, is not well understood.

**Transcriptomic analysis of microarray data from Hnf4a tissue-specific knockouts revealed that distinct subsets of Phase I, Phase II and Phase III genes were affected in developing liver, colon, intestine and pancreas**

There is no mouse model with a kidney-specific deletion of Hnf4a; this may reflect a role very early in kidney development (prior to proximal tubule morphogenesis) (Kanazawa et al., 2010), in addition to the later postnatal role in proximal tubule DME regulation that we have focused on here. Nevertheless, this nuclear receptor has been deleted in five other developing and mature tissues; the knockout tissue has been subjected to microarray analysis. Together, these tissues express most of the DMEs from our original curated list. Therefore, it is possible to determine which of the DMEs has direct or indirect regulation of its expression by Hnf4a; to the extent that these DMEs overlap with the set identified above in the developing proximal tubule of the kidney, it may be possible to infer a high probability of transcriptional regulation by Hnf4a in the kidney.

To this end, we analyzed the published microarray expression data from five tissues with specific Hnf4a knockout models: E18.5 liver (Battle et al., 2006), E18.5 colon (Garrison et al., 2006), adult colon (Darsigny et al., 2009), adult small intestine, and adult isolated B-islet cells (Boj et al., 2010). Of note, the consequence of deletion of Hnf4a has varying effects on the different tissues. Hnf4a is required for epithelialization and functional differentiation of hepatocytes; as a result, the consequences of removing this gene in the liver are severe, leading to embryonic lethality. The differentiation and function of the colonic epithelium is altered, but this does not prevent the animal from reaching adulthood. While the small intestine also expresses Hnf4a, its deletion apparently has minimal morphological consequences (Babeu et al.,

2009). Finally, B-islet cells lacking Hnf4a exhibit mild phenotypic and functional consequences, despite marked differences in the transcriptome.

We compared Hnf4a <sup>-/-</sup> tissues to matched wild type samples and identified significantly changing ( $p < 0.05$ ,  $FC > 1.3$ ) probe sets in each tissue (Fig. 4A). We then assembled a list of DMEs that were differentially-expressed as a result of Hnf4a deletion in at least one tissue. The list includes 203 regulated DMEs (96 Phase I enzymes, 79 Phase II enzymes, and 28 Phase III transporters). Liver experienced the most changes in DME expression; followed by adult colon, B-islets, small intestine and embryonic colon, respectively. Of note, 156 of the 203 DMEs downstream of Hnf4a regulation in at least one knockout tissue are expressed in either embryonic or adult mouse proximal tubules, and they thus represent a group of DMEs potentially regulated in the proximal tubule by Hnf4a under either basal or stimulated conditions [Fig. 4B, Supplemental Table 4 (detailed view of Figure 4B)].

Interestingly, not a single DME gene was significantly changing in more than three tissues. In most cases, genes affected in more than one tissue were changing in the same direction. However, there are examples of the same gene being regulated in opposite directions in different tissues. Of the 203 affected DMEs, 12 changed in three tissues, 47 in two, and 144 were specifically regulated in a single tissue. On the other hand, expression of related gene family members in different tissues was frequently observed. These findings further supported that Hnf4a plays an important role in transcriptional regulation of DMEs in specific tissues during development, as well as in mature tissues. However, based on the large divergence of affected downstream targets, Hnf4a-mediated regulation appears to highly depend on cellular context.

**Hepatocyte nuclear factor 4a plays a major role in establishing and maintaining transcriptional enhancer elements that regulate DME genes in the proximal tubule**

To gain more insight into proximal tubule-specific regulation, we used ChIP-seq to determine the co-localization of Hnf4a in rat proximal tubule cells at the three earlier-identified stages – pre-natal differentiation, maturation and adulthood. To represent these transitions, we selected the following three time points: 20 days post coitum (E20), 2 weeks old (P13) and adult (8 weeks). By E20, late differentiation events are occurring, although new nephrons are still being formed; importantly, at this time point, the kidney is naïve to the influences of birth and the extra-uterine environment. At P13, new nephrons are no longer being formed (Larsson, 1975), but the transcriptional profile or functional capacity has not yet reached mature levels (Sweeney et al., 2011). Finally, the proximal tubule reaches maturity after puberty, which occurs around 4-6 weeks in rodents. In the kidney, Hnf4a expression has been reported in condensed mesenchyme (Kanazawa et al., 2010), and in segments of nephron progenitor structures throughout all of nephrogenesis (Kanazawa et al., 2009), though ultimately its expression becomes restricted to the proximal tubule. Thus, even when using chromatin prepared from the entire population of kidney cells, Hnf4a-binding can be attributed to Hnf4a-expressing cells.

Figure 5A quantifies general results of Hnf4a ChIP-seq, along with the p300 data. At E20, Hnf4a occupancy was detected at 38,145 sites, revealing robust activity during late embryogenesis. During maturation, at P13, Hnf4a was detected at 52,541 locations. In mature proximal tubules, 79,871 sites containing Hnf4a were found (Fig. 5A). Thus, the number of Hnf4a binding locations in proximal tubules more than doubles from initial differentiation until reaching maturity. Subsequently, Hnf4a-mediated transcriptional regulation is expected to change as a result of gained or lost binding events. Figure 6 shows representative screenshots of binding events and peak overlap from all four ChIP-seq experiments. Perhaps one of the most striking findings was the high level Hnf4a and p300 co-localization (Fig. 5B). At E20, 14,966

Hnf4a peaks, 39% of all peaks, were at locations that are occupied by p300 in mature proximal tubules. At P13, the number goes up to 20,209, or 38% of total Hnf4a peaks at this age. Finally, in the adult, 25,171 Hnf4a binding locations, or 32% of all peaks, are co-occupied by p300. This suggests that Hnf4a might directly recruit p300, thus establishing cis-regulatory enhancer elements. Furthermore, the high level of Hnf4a-containing enhancer elements in adult proximal tubules implies a large role for Hnf4a in establishing gene expression profiles in these cells, exemplified by a specific DME repertoire.

We also examined differential binding of Hnf4a at the three developmental stages (prenatal, postnatal, adult). Peak overlap is one possible approach; however, this fails to differentiate between significant changes and borderline differences that affect peak calling. Instead, we identified peaks with at least 4-fold changes in tag density at different time points (Fig. 5B). Of 38,145 peaks present at E20, 6,285 were significantly downregulated or completely lost by P13. Conversely, only 1,856 of 52,541 peaks present at P13 were downregulated/absent in adult proximal tubules. Both transitions experienced comparable numbers of upregulated Hnf4a occupancy, with 13,432 upregulated sites from E20 to P13, and 17,706 upregulated sites from P13 to Adult (Fig. 5B). Interestingly, motif analysis of Hnf4a peaks revealed that Hnf1a binding motifs were enriched at Hnf4a binding sites in P13 and adult proximal tubules, but not at E20 (data not shown).

Thus, there are substantial changes in Hnf4a binding during pre and postnatal development. Based on Hnf4a occupancy throughout proximal tubule development and maturation, it is clear that it plays important roles in regulation of the proximal tubule transcriptome. We then focused in on peaks near or within DMEs, which are likely to regulate that locus. We found that most of the expressed DMEs were bound by Hnf4a near or within the

genes, many of which contained peaks near the TSS. While there was a notable degree of differential binding, it was more common to see peaks that were present at E20 become more enriched and formation of new peaks as proximal tubule cells mature.

Part of Hnf4a-mediated regulation of DMEs in the proximal tubule may depend on exerting specific effects on other DME transcriptional regulators, rather than directly targeting DMEs. It appears that this is plausible – based on Hnf4a binding at relevant nuclear receptors. Very high Hnf4a enrichment was observed along the Ppara gene locus, a nuclear receptor predicted earlier (Fig. 1) to regulate a subset of DMEs in the PT. In contrast, Pparg had a very low number of binding events, consistent with lack of expression (Fig. 6A). An interesting observation was a modest presence of Hnf4a co-localization around genes that are not basally expressed in the proximal tubule, sometimes even directly at the promoter. Conversely, all predicted DME transcriptional regulators included in Figure 1 had high Hnf4a enrichment at multiple sites, often including the promoter.

### **Administration of an Hnf4a small molecule antagonist in an ex vivo kidney organ culture model markedly attenuated the expression of representative Phase I, II and III DMEs**

Our findings support the view that Hnf4a plays an important role in transcriptional regulation of DMEs during kidney differentiation and maturation. There is currently no reported mouse model with kidney-specific ablation of Hnf4a to test this in vivo. Instead, we utilized a recently developed small molecule compound that specifically antagonizes Hnf4a activity (Kiselyuk et al., 2012). With this compound, we tested the effect of Hnf4a downregulation in embryonic kidney organ culture (grown for 6.5 days to allow nascent PT formation), which recapitulates many characteristics of proximal tubule differentiation, including the acquisition of



organic anion transport mediated by Oat1 and Oat3 (Sweet et al., 2006). Based on in vitro and in vivo knockout data, this is generally believed to be the main pathway for kidney elimination of many common drugs (eg. antibiotics, antivirals, diuretics, nonsteroidal anti-inflammatory drugs) and toxins (eg. mercury conjugates) (Torres et al., 2011; VanWert et al., 2010). This pathway has received increased attention given new FDA guidelines, and its role in neonatal drug handling is of considerable interest.

Hnf4a inhibition in kidney culture caused differential expression, mainly (but not exclusively) downregulation, of many representative Phase I, II and III drug-metabolizing genes (Fig. 7). Targets were selected based on exhibiting PT-specific expression in the kidney (Fig. 2), known expression in embryonic proximal tubules, presence of Hnf4a binding near or within the gene, and in some cases because they were regulated by Hnf4a in other tissues (Fig. 4). Some genes exhibited a dose-dependent effect in downregulation, while expression of others was maximally downregulated with the lower antagonist concentration, without further decrease at a higher concentration. Of the genes tested, several did not change or were upregulated, indicating that the antagonist had a selective effect on only a certain subset of PT DMEs, presumably those regulated by Hnf4a. This role of Hnf4a was further explored below by lentiviral transduction into cells.

### **Overexpression of Hnf1a and Hnf4a in mouse embryonic fibroblasts induces expression of proximal tubule Phase I, II and III DMEs**

To further explore the role of Hnf4a, and the highest associated co-regulator Hnf1a, we examined the capacity of these factors to induce expression of DMEs highly expressed in the proximal tubule in MEFs. Using lentiviral transduction, mouse Hnf1a and Hnf4a cDNA with

downstream EGFP was introduced either individually or in combination into primary fibroblasts derived from E16.5 mouse embryos. Approximately 75% transduction efficiency was routinely achieved (Fig. 8A). As shown in Figure 8B, transduction of Hnf1a did not induce expression of endogenous Hnf4a, or vice versa; however, both genes are expressed within the cell population upon transduction of both factors. Unaltered expression of p53 suggests the lack of apoptotic response from the genomic integrations or overexpressed proteins. As can be seen in Figures 8C and 8D, expression of a limited number of DMEs and epithelial markers [E-cadherin (Cdh1) and Tight junction protein 1 (Tjp1)] was induced to different extents by Hnf1a or Hnf4a alone. Importantly, expression of many genes was dependent on the presence of both Hnf4a and Hnf1a. We then sought to determine if the function of some genes relevant to drug metabolism by the proximal tubule upon transduction of Hnf1a and Hnf4a was consistent with their mRNA expression. To this end, we examined the ability of transduced MEFs to take up 6-Carboxyfluorescein in a probenecid-sensitive manner, which is a classical indicator of Slc22a6 (Oat1) function. Oat1 is one of the major drug, toxin and metabolite transporters in the developing and mature proximal tubule (Ahn and Nigam, 2009; Eraly et al., 2008; Eraly et al., 2006; Lopez-Nieto et al., 1997; Wu et al., 2011). As shown in Figure 8E, upon expression of Hnf1a and Hnf4a, transduced MEFs gained the ability to accumulate 6-CF through a functional specific transport mechanism (via Oat1). Although the bulk of the evidence suggests that the MEFs differentiated toward PT-like cells, without an exhaustive analysis of other tissue markers we cannot exclude the possibility of characteristics overlapping with other cell types expressing Hnf4a and Hnf1a.

## Discussion:

Even in such a well-studied organ as the liver, the developmental maturation of drug handling and metabolism—which depends on Phase I and Phase II enzymes as well as Phase III transporters – remains incompletely understood. Even less is known about other developing organs, including the kidney. In order to properly dose neonates and children, and to diminish adverse effects from drugs and environmental toxins, it is important to understand the molecular basis of drug and toxin handling. In this study, we have combined systems, molecular and cellular biology approaches to show that Hnf1a and Hnf4a cooperate to play a major role in the transcriptional initiation and maturation of genes in the developing and postnatal proximal tubule involved in Phase I, II and III drug metabolism.

In order to approach the problem of prenatal and postnatal proximal tubule maturation, we began with a broad approach, employing microarray data to study a broadly-defined set of DMEs (Table 1) in the context of proximal tubule expression. Network analysis of transcriptional profiles of DMEs in nascent and mature mouse proximal tubules suggested roles for a small set of transcription factors which may be orchestrating the expression of Phase I, II and III genes in the proximal tubule (Fig. 1C). Further analysis of a time-series of expression in rat kidneys not only defined the dynamics of DME expression but revealed a significant role of DMEs in defining the proximal tubule-specific transcriptome in the kidney. This finding suggested that lineage-determining factors associated with PT-specific enhancers on a global scale would likely regulate expression of DMEs.

In our studies, transcription factor motifs present in enhancer regions marked by p300 suggested that Hnf4a, along with Hnf1a – a known transcriptional regulator of proximal tubule

function (Pontoglio et al., 1996), might be the major regulators of PT expression of DMEs. We chose p300 over histone modifications to characterize enhancers due to two main advantages: 1) p300 cannot bind DNA directly, thus peaks represent presence of DNA-binding factors that recruited p300; 2) p300 peaks are more localized than histone modification, facilitating recognition of binding motifs of responsible targeting factors. Nevertheless, it is possible that additional information could be gained by examining other enhancer elements that lack p300 co-localization in future studies, which may offer additional clues regarding the contribution of other transcription factors, potentially including those identified in Figure 1C.

Although there is good evidence that HNF4a can regulate transcription of a number of DMEs in the liver, there has been little direct evidence of this in the PT. A kidney-specific knockout has not been reported thus far, possibly because of an early defect in nephrogenesis that precedes PT differentiation (Kanazawa et al., 2010). Nevertheless, by restricting the list of targets downstream of Hnf4a in other tissues to those expressed in the prenatal or mature PT, we were able to suggest a subset of DMEs that are potentially basally or constitutively regulated by HNF4a in the proximal tubule (Fig. 4B, Supplemental Table 4). This subset had many Phase I, II and III genes known to carry out important reactions involved in drug metabolism. However, while many of these genes are likely to be regulated by Hnf4a in the PT, Figure 4A shows that there is a substantial portion of targets regulated in only a single tissue. Furthermore, it is important to note that some very important DMEs expressed in the PT fail to be detected by expression microarrays in these other tissues, such as *Oat1* and *Oat3*.

Given the evidence strongly suggesting that Hnf4a might be playing a critical role in DME regulation in the proximal tubule, and the tissue-specific nature of this regulation, we decided to characterize the genome wide co-localization of Hnf4a in the developing kidney in-

vivo at three distinct developmental stages – prenatal differentiation, postnatal maturation and adulthood. The time points chosen to represent these stages (E20, P13 and Adult) were chosen mainly based on analysis shown in Figure 2. However, the selection of time points was also supported by prior analysis of time series microarray expression data from developing and adult kidneys (Tsigelny et al., 2008), as well as functional correlations such as the in vivo ability to transport classical organic anion substrates such as para-aminohippurate, which may be viewed as a surrogate for the capacity of the kidney to eliminate drugs and toxins by the Oat1 transporter (Sweeney et al., 2011).

As mentioned, it has been previously shown that Hnf4a plays a key role in morphogenesis during kidney development – cap mesenchyme survival (Kanazawa et al., 2010) – which occurs far before the differentiation and development of the PT; the role of Hnf4a in the maturation of the proximal tubule during late prenatal and postnatal development remained poorly defined. By using a recently developed small molecule antagonist which has been shown to selectively inhibit Hnf4a (Kiselyuk et al., 2012), we were able to explore the consequences of Hnf4a downregulation in early proximal tubules in 7 day organ culture, which serves as a model for kidney development. These have been shown to express Slc22 transporters such as Oat1 and Oat3 and eventually become capable of organic anion transport function (Sweet et al., 2006). As predicted, Hnf4a inhibition by the compound (but not a structurally similar inactive compound) resulted in markedly diminished expression of important Phase I, II and III DMEs, including Oat1 and Oat3, suggesting that Hnf4a is required to maintain basal expression of many functionally important DMEs in the PT. Expression of a small group of DMEs, however, was unchanged or upregulated in response to the Hnf4a antagonist, potentially indicating reversal of Hnf4a-mediated repression. These experiments supported a key role for DME regulation by

Hnf4a in the whole organ culture. Nevertheless, we also sought to prove this directly by lentiviral transduction of Hnf4a and Hnf1a into MEFs.

Overexpression of Hnf1a and Hnf4a in MEFs provided the final clues to help postulate a working model for the role of Hnf4a in the transcriptional regulation of PT development and function. For all of the tested genes aside from *Gsta1* and *Slc47a1* (*Mate1*), Hnf4a alone failed to induce expression of PT DME genes. Since we have also presented substantial data suggesting the involvement of Hnf1a (Fig. 1B,C and Fig. 3B), we also tested Hnf1a by itself. Hnf1a alone also showed little potential to induce expression of PT DMEs in MEFs. We were surprised to find that neither factor was able to induce the expression of the other one by itself, considering multiple lines of evidence for cross-regulation, and the fact that a set of clinically-relevant Phase III transporters – *Slc22a6*, *Slc22a7*, *Slc22a8* and *Slco1a1* – are significantly downregulated in Hnf1a *-/-* mature kidneys (Maher et al., 2006). Remarkably, when introduced in combination, Hnf4a and Hnf1a were able to induce robust expression of many predicted DME targets in the PT (Fig. 8C).

Taking all of our findings into consideration, we suggest the following model. The primary role of Hnf4a is to set up basal and constitutive cis-regulatory enhancer elements, which then become accessible to other co-regulators. Considering the fact that Hnf4a plays important but varying roles in the liver and other tissues, chromatin state and other factors are likely to be important in helping establish tissue-specific binding profiles of Hnf4a. Hnf1a and other co-regulators may establish an additional layer of specificity in a combinatorial fashion, leading to the appropriate expression profiles in different tissues. Other co-regulators might involve other members of the nuclear receptor family, which are known to play important roles in regulating metabolic function in the proximal tubule, as well as transcriptional repressors. Of note, a

generic nuclear receptor binding motif was highly abundant and enriched within Hnf4a peaks (data not shown). It might be possible that nuclear receptors regulate target genes via Hnf4a-established enhancers, either by binding nearby or by competing for lower-affinity binding sites. In this context, it is worth pointing out that there were Hnf4a peaks at non-expressed genes that might be important in later proximal tubule function (eg. Car (Nr1i3), Pxr (Nr1i2)); some of these may be poised enhancers, perhaps requiring stimulation by other transcription factors (including those implicated in Figure 1C) in later life or during periods of stress. These nuclear receptors are thought to act as ligand-dependent “sensors” (Rosenfeld et al., 2006). According to the Remote Sensing and Signaling Hypothesis, “drug” transporters such as those regulated by nuclear receptors play a role in regulating inter-organ communication in normal physiology, after perturbation of homeostasis and possibly during development; in this context, it is conceivable that HNF4a and other nuclear receptors play a key role in the sensing specific metabolic alterations, leading to the necessary changes in transporter and DME expression.

In summary, we have shown that Hnf4a is required for basal expression of DMEs in the proximal tubule. Furthermore, we demonstrated that, together, Hnf1a and Hnf4a are sufficient to induce the expression of representative proximal tubule Phase I, II and III drug-metabolizing genes, further supporting their roles in DME regulation in the developing PT. The data from this study should prove helpful in defining the steps involved in the transcriptional maturation of the proximal tubule that involve Hnf4a, Hnf1a and other transcription factors as they relate to the expression of drug transporters and Phase I/II drug-metabolizing enzymes.

## Acknowledgments:

We thank Dr. Fred Levine and Seung-Hee Lee for helpful discussions and for providing the Hnf4a antagonist BI6015 and control compound BI6018. We would also like to thank Dr. Lijian Hui for providing the lentiviral plasmids containing Hnf4a or Hnf1a cDNA inserts.



## Authorship Contributions:

*Participated in research design:* Martovetsky, Tee, Nigam

*Conducted experiments:* Martovetsky

*Contributed new reagents or analytic tools:* Martovetsky, Tee, Nigam

*Performed data analysis:* Martovetsky

*Wrote or contributed to the writing of the manuscript:* Martovetsky, Nigam

## References

- Ahn, S. Y. and Nigam, S. K.** (2009). Toward a systems level understanding of organic anion and other multispecific drug transporters: a remote sensing and signaling hypothesis. *Mol Pharmacol* **76**, 481-90.
- Aleksunes, L. M. and Klaassen, C. D.** (2012). Coordinated regulation of hepatic phase I and II drug-metabolizing genes and transporters using AhR-, CAR-, PXR-, PPARalpha-, and Nrf2-null mice. *Drug Metab Dispos* **40**, 1366-79.
- Babeu, J. P., Darsigny, M., Lussier, C. R. and Boudreau, F.** (2009). Hepatocyte nuclear factor 4alpha contributes to an intestinal epithelial phenotype in vitro and plays a partial role in mouse intestinal epithelium differentiation. *Am J Physiol Gastrointest Liver Physiol* **297**, G124-34.
- Battle, M. A., Konopka, G., Parviz, F., Gagli, A. L., Yang, C., Sladek, F. M. and Duncan, S. A.** (2006). Hepatocyte nuclear factor 4alpha orchestrates expression of cell adhesion proteins during the epithelial transformation of the developing liver. *Proc Natl Acad Sci U S A* **103**, 8419-24.
- Boj, S. F., Petrov, D. and Ferrer, J.** (2010). Epistasis of transcriptomes reveals synergism between transcriptional activators Hnf1alpha and Hnf4alpha. *PLoS Genet* **6**, e1000970.
- Brunskill, E. W., Aronow, B. J., Georgas, K., Rumballe, B., Valerius, M. T., Aronow, J., Kaimal, V., Jegga, A. G., Yu, J., Grimmond, S. et al.** (2008). Atlas of gene expression in the developing kidney at microanatomic resolution. *Dev Cell* **15**, 781-91.
- Burckhardt, G. and Burckhardt, B. C.** (2011). In vitro and in vivo evidence of the importance of organic anion transporters (OATs) in drug therapy. *Handb Exp Pharmacol*, 29-104.
- Coffinier, C., Barra, J., Babinet, C. and Yaniv, M.** (1999). Expression of the vHNF1/HNF1beta homeoprotein gene during mouse organogenesis. *Mech Dev* **89**, 211-3.
- Darsigny, M., Babeu, J. P., Dupuis, A. A., Furth, E. E., Seidman, E. G., Levy, E., Verdu, E. F., Gendron, F. P. and Boudreau, F.** (2009). Loss of hepatocyte-nuclear-factor-4alpha affects colonic ion transport and causes chronic inflammation resembling inflammatory bowel disease in mice. *PLoS One* **4**, e7609.
- Dunham, I., Kundaje, A., Aldred, S. F., Collins, P. J., Davis, C. A., Doyle, F., Epstein, C. B., Frietze, S., Harrow, J., Kaul, R. et al.** (2012). An integrated encyclopedia of DNA elements in the human genome. *Nature* **489**, 57-74.
- Eraly, S. A., Vallon, V., Rieg, T., Gangoiti, J. A., Wikoff, W. R., Siuzdak, G., Barshop, B. A. and Nigam, S. K.** (2008). Multiple organic anion transporters contribute to net renal excretion of uric acid. *Physiol Genomics* **33**, 180-92.
- Eraly, S. A., Vallon, V., Vaughn, D. A., Gangoiti, J. A., Richter, K., Nagle, M., Monte, J. C., Rieg, T., Truong, D. M., Long, J. M. et al.** (2006). Decreased renal organic anion secretion and plasma accumulation of endogenous organic anions in OAT1 knock-out mice. *J Biol Chem* **281**, 5072-83.

- Gallegos, T. F., Martovetsky, G., Kouznetsova, V., Bush, K. T. and Nigam, S. K.** (2012). Organic anion and cation SLC22 "drug" transporter (Oat1, Oat3, and Oct1) regulation during development and maturation of the kidney proximal tubule. *PLoS One* **7**, e40796.
- Garrison, W. D., Battle, M. A., Yang, C., Kaestner, K. H., Sladek, F. M. and Duncan, S. A.** (2006). Hepatocyte nuclear factor 4alpha is essential for embryonic development of the mouse colon. *Gastroenterology* **130**, 1207-20.
- Giacomini, K. M., Huang, S. M., Tweedie, D. J., Benet, L. Z., Brouwer, K. L., Chu, X., Dahlin, A., Evers, R., Fischer, V., Hillgren, K. M. et al.** (2010). Membrane transporters in drug development. *Nat Rev Drug Discov* **9**, 215-36.
- Heintzman, N. D., Hon, G. C., Hawkins, R. D., Kheradpour, P., Stark, A., Harp, L. F., Ye, Z., Lee, L. K., Stuart, R. K., Ching, C. W. et al.** (2009). Histone modifications at human enhancers reflect global cell-type-specific gene expression. *Nature* **459**, 108-12.
- Heintzman, N. D., Stuart, R. K., Hon, G., Fu, Y., Ching, C. W., Hawkins, R. D., Barrera, L. O., Van Calcar, S., Qu, C., Ching, K. A. et al.** (2007). Distinct and predictive chromatin signatures of transcriptional promoters and enhancers in the human genome. *Nat Genet* **39**, 311-8.
- Heinz, S., Benner, C., Spann, N., Bertolino, E., Lin, Y. C., Laslo, P., Cheng, J. X., Murre, C., Singh, H. and Glass, C. K.** (2010). Simple combinations of lineage-determining transcription factors prime cis-regulatory elements required for macrophage and B cell identities. *Mol Cell* **38**, 576-89.
- Huang, P., He, Z., Ji, S., Sun, H., Xiang, D., Liu, C., Hu, Y., Wang, X. and Hui, L.** (2011). Induction of functional hepatocyte-like cells from mouse fibroblasts by defined factors. *Nature* **475**, 386-9.
- Kanazawa, T., Konno, A., Hashimoto, Y. and Kon, Y.** (2009). Expression of hepatocyte nuclear factor 4alpha in developing mice. *Anat Histol Embryol* **38**, 34-41.
- Kanazawa, T., Konno, A., Hashimoto, Y. and Kon, Y.** (2010). Hepatocyte nuclear factor 4 alpha is related to survival of the condensed mesenchyme in the developing mouse kidney. *Dev Dyn* **239**, 1145-54.
- Kiselyuk, A., Lee, S. H., Farber-Katz, S., Zhang, M., Athavankar, S., Cohen, T., Pinkerton, A. B., Ye, M., Bushway, P., Richardson, A. D. et al.** (2012). HNF4alpha antagonists discovered by a high-throughput screen for modulators of the human insulin promoter. *Chem Biol* **19**, 806-18.
- Larsson, L.** (1975). The ultrastructure of the developing proximal tubule in the rat kidney. *J Ultrastruct Res* **51**, 119-39.
- Lash, L. H., Putt, D. A. and Cai, H.** (2008). Drug metabolism enzyme expression and activity in primary cultures of human proximal tubular cells. *Toxicology* **244**, 56-65.
- Lazzaro, D., De Simone, V., De Magistris, L., Lehtonen, E. and Cortese, R.** (1992). LFB1 and LFB3 homeoproteins are sequentially expressed during kidney development. *Development* **114**, 469-79.

**Lee, J. S., Ward, W. O., Liu, J., Ren, H., Vallanat, B., Delker, D. and Corton, J. C.** (2011). Hepatic xenobiotic metabolizing enzyme and transporter gene expression through the life stages of the mouse. *PLoS One* **6**, e24381.

**Lohr, J. W., Willsky, G. R. and Acara, M. A.** (1998). Renal drug metabolism. *Pharmacol Rev* **50**, 107-41.

**Lopez-Nieto, C. E., You, G., Bush, K. T., Barros, E. J., Beier, D. R. and Nigam, S. K.** (1997). Molecular cloning and characterization of NKT, a gene product related to the organic cation transporter family that is almost exclusively expressed in the kidney. *J Biol Chem* **272**, 6471-8.

**Maher, J. M., Slitt, A. L., Callaghan, T. N., Cheng, X., Cheung, C., Gonzalez, F. J. and Klaassen, C. D.** (2006). Alterations in transporter expression in liver, kidney, and duodenum after targeted disruption of the transcription factor HNF1alpha. *Biochem Pharmacol* **72**, 512-22.

**Miyoshi, H., Blomer, U., Takahashi, M., Gage, F. H. and Verma, I. M.** (1998). Development of a self-inactivating lentivirus vector. *J Virol* **72**, 8150-7.

**Morrissey, K. M., Wen, C. C., Johns, S. J., Zhang, L., Huang, S. M. and Giacomini, K. M.** (2012). The UCSF-FDA TransPortal: a public drug transporter database. *Clin Pharmacol Ther* **92**, 545-6.

**Nagle, M. A., Truong, D. M., Dnyanmote, A. V., Ahn, S. Y., Eraly, S. A., Wu, W. and Nigam, S. K.** (2011). Analysis of three-dimensional systems for developing and mature kidneys clarifies the role of OAT1 and OAT3 in antiviral handling. *J Biol Chem* **286**, 243-51.

**Nigam, S. K. and Bhatnagar, V.** (2013). How Much Do We Know About Drug Handling by SLC and ABC Drug Transporters in Children? *Clin Pharmacol Ther* **94**, 27-9.

**Nigam, S. K., Bush, K. T. and Bhatnagar, V.** (2007). Drug and toxicant handling by the OAT organic anion transporters in the kidney and other tissues. *Nat Clin Pract Nephrol* **3**, 443-8.

**Pontoglio, M., Barra, J., Hadchouel, M., Doyen, A., Kress, C., Bach, J. P., Babinet, C. and Yaniv, M.** (1996). Hepatocyte nuclear factor 1 inactivation results in hepatic dysfunction, phenylketonuria, and renal Fanconi syndrome. *Cell* **84**, 575-85.

**Rosenfeld, M. G., Lunyak, V. V. and Glass, C. K.** (2006). Sensors and signals: a coactivator/corepressor/epigenetic code for integrating signal-dependent programs of transcriptional response. *Genes Dev* **20**, 1405-28.

**Sekiya, S. and Suzuki, A.** (2011). Direct conversion of mouse fibroblasts to hepatocyte-like cells by defined factors. *Nature* **475**, 390-3.

**Shen, Y., Yue, F., McCleary, D. F., Ye, Z., Edsall, L., Kuan, S., Wagner, U., Dixon, J., Lee, L., Lobanenkov, V. V. et al.** (2012). A map of the cis-regulatory sequences in the mouse genome. *Nature* **488**, 116-20.

**Sweeney, D. E., Vallon, V., Rieg, T., Wu, W., Gallegos, T. F. and Nigam, S. K.** (2011). Functional maturation of drug transporters in the developing, neonatal, and postnatal kidney. *Mol Pharmacol* **80**, 147-54.

**Sweet, D. H., Eraly, S. A., Vaughn, D. A., Bush, K. T. and Nigam, S. K.** (2006). Organic anion and cation transporter expression and function during embryonic kidney development and in organ culture models. *Kidney Int* **69**, 837-45.

**Torres, A. M., Dnyanmote, A. V., Bush, K. T., Wu, W. and Nigam, S. K.** (2011). Deletion of multispecific organic anion transporter Oat1/Slc22a6 protects against mercury-induced kidney injury. *J Biol Chem* **286**, 26391-5.

**Tsigelny, I. F., Kouznetsova, V. L., Sweeney, D. E., Wu, W., Bush, K. T. and Nigam, S. K.** (2008). Analysis of metagene portraits reveals distinct transitions during kidney organogenesis. *Sci Signal* **1**, ra16.

**Van den Bosch, H. M., Bunger, M., de Groot, P. J., van der Meijde, J., Hooiveld, G. J. and Muller, M.** (2007). Gene expression of transporters and phase I/II metabolic enzymes in murine small intestine during fasting. *BMC Genomics* **8**, 267.

**VanWert, A. L., Gionfriddo, M. R. and Sweet, D. H.** (2010). Organic anion transporters: discovery, pharmacology, regulation and roles in pathophysiology. *Biopharm Drug Dispos* **31**, 1-71.

**Visel, A., Blow, M. J., Li, Z., Zhang, T., Akiyama, J. A., Holt, A., Plajzer-Frick, I., Shoukry, M., Wright, C., Chen, F. et al.** (2009). ChIP-seq accurately predicts tissue-specific activity of enhancers. *Nature* **457**, 854-8.

**Wright, J., Morales, M. M., Sousa-Menzes, J., Ornellas, D., Sipes, J., Cui, Y., Cui, I., Hulamm, P., Cebotaru, V., Cebotaru, L. et al.** (2008). Transcriptional adaptation to Clcn5 knockout in proximal tubules of mouse kidney. *Physiol Genomics* **33**, 341-54.

**Wu, W., Dnyanmote, A. V. and Nigam, S. K.** (2011). Remote communication through solute carriers and ATP binding cassette drug transporter pathways: an update on the remote sensing and signaling hypothesis. *Mol Pharmacol* **79**, 795-805.

**Xi, H., Shulha, H. P., Lin, J. M., Vales, T. R., Fu, Y., Bodine, D. M., McKay, R. D., Chenoweth, J. G., Tesar, P. J., Furey, T. S. et al.** (2007). Identification and characterization of cell type-specific and ubiquitous chromatin regulatory structures in the human genome. *PLoS Genet* **3**, e136.

## Footnotes:

The work was supported by the National Institutes of Health National Institute of Child Health and Human Development [Grant U54-HD07160], the National Institutes of Health National Institute of General Medical Sciences [Grant RO1-GM098449 and GM104098], and Alberta Children's Hospital Foundation establishment grant.

Contact for reprint requests: Sanjay K. Nigam

University of California, San Diego, 9500 Gilman Drive, MC0693, La Jolla, CA 92093

E-mail: [snigam@ucsd.edu](mailto:snigam@ucsd.edu)

## Figure Legends:

### **Figure 1. DMEs are dynamically regulated in proximal tubule development.**

A) Of 297 DMEs expressed in either embryonic (E15.5) or adult mouse proximal tubules, 170 were significantly changing ( $p < 0.05$ ) at least 2-fold. B) Expression of IPA-predicted upstream regulators of DMEs in mouse PTs. \*Although *Hnfla* expression in the proximal tubule is well documented (Coffinier et al., 1999; Lazzaro et al., 1992; Pontoglio et al., 1996), there appeared to be issues with probe sets on the mouse chip; therefore, an expression value (not to scale) has been adopted from another publically available source – the Rat Proximal Tubule Transcriptome Database (<http://dir.nhlbi.nih.gov/papers/lkem/pttr/>). Constitutive androstane receptor (Car) was not detected in any of the datasets. C) Ingenuity Pathway Analysis-predicted network of DME transcriptional regulation in proximal tubule development and maturation.

### **Figure 2. DMEs contribute to proximal tubule gene expression and cellular identity.**

While DMEs make up less than 3% of the total annotated genes, DMEs account for over 12% of proximal tubule-enriched gene expression in the rat kidney throughout development [subset of published data (Tsigelny et al., 2008)], based on lists of enriched genes in E15.5 mouse proximal tubules, which were adapted from a published study (Brunskill et al., 2008). DMEs are highlighted in green (35/280 genes).

### **Figure 3. P300 ChIP-seq in adult rat kidney cortex reveals *Hnf4a* as the top transcriptional regulator in proximal tubules.**

A) Screenshots of p300 peaks (tags per bp normalized to input). P300 is highly enriched at the *Oat1*, *Oat3* and *Mate1* loci, three highly expressed drug transporters which are specific to the proximal tubule in the kidney. *Aldh3a2*, which is expressed in the PT, had a strong peak at the promoter; conversely, *Aldh3a1* and *Mate2*, which are not

expressed in the PT, exhibited minimal p300 co-localization. There were multiple peaks at the Hnf1a locus, but none at Nr1i3, which is consistent with the finding that Hnf1a but not Car are expressed in the PT (Fig. 1B). B) Motif analysis of promoter-distal p300 peaks revealed that the two highest enriched transcription factor binding motifs matched those of Hnf4a and Hnf1a. The motif for the ubiquitous insulator CTCF was also enriched around p300 binding sites, which is consistent with previous studies.

**Figure 4. Hnf4a is highly involved in tissue specific expression of DMEs.** A) Comparison of significantly changing ( $FC > 1.3$ ,  $p < 0.05$  using uncorrected t-test) probe sets in four tissues (E18.5 liver, E18.5 colon, adult colon, adult B-islet cells) with conditional Hnf4a deletion. B) Heatmap of significantly changing DME genes from same four tissues in panel A, in addition to small intestine, matched to expression levels in embryonic and adult mouse proximal tubules. Rows are color-coded for Phase I, II and III with yellow, green and blue, respectively, and split into those expressed in the pre and/or postnatal PT (on top) and those that are not expressed in the PT (bottom). Their corresponding expression in E15.5 and adult PTs is shown on the left (red = high expression, light = low expression, white = not detected). Genes are sorted within Phase I, II and III groups by expression levels in adult proximal tubules. To the right, differential expression in corresponding tissues is depicted. 156 of 203 differentially expressed DMEs were found to be expressed in proximal tubules. The detailed list is included in Supplemental Table 4.

**Figure 5. Quantitation and characterization of ChIP-seq reads.** A) General measures of ChIP-seq data. B) Pairwise quantitation of overlapping peaks between all four ChIP experiments (top), as well as differentially-bound Hnf4a peaks with higher signal in column relative to row (bottom).



**Figure 6. Hnf4a regulates PT gene expression throughout kidney development and**

**maturation.** A) Screenshots of peaks from all four ChIP-seq experiments. Oat1 and Oat3, two major drug transporters in the proximal tubule, accumulate Hnf4a binding events throughout development. While there was minimal colocalization of Hnf4a and p300 at the Pparg locus, there were multiple binding events associated with Ppara, which was implicated in Fig. 1C as a regulator of DME expression in the PT. B) Schematic representing the overlap of all possible combinations of peaks. C) Proportionally-scaled heatmap of tag densities of five representative sub-categories highlighted in Fig. 5B.

**Figure 7. Antagonism of Hnf4a in embryonic rat kidney culture leads to differential effects**

**on Phase I, II and III DMEs.** E13.5 rat kidneys were cultured on Transwell filters for 6.5 days, and treated with a small molecule antagonist of Hnf4a or an analogous inactivated compound for 12 hours. A) Schematic of embryonic kidney culture on Transwell filters. B) Example of embryonic kidney cultured for 7 days (red – Dolichos Biflorous; green – E-cadherin; blue – DAPI). C) Changes in expression in whole rat embryonic kidneys in response to Hnf4a inhibition with a small molecule antagonist, relative to treatment with carrier alone (DMSO).

**Figure 8. Hnf4a and Hnf1a induce expression of proximal tubule DMEs.**

A) Flow cytometry was used to quantify transduction efficiency, which was routinely around 70-80% as judged by the fraction GFP+ live cells. B) Uninfected cells do not express Hnf1a or Hnf4a, while lentiviral transduction leads to expression of the respective genes. Unaltered p53 expression levels indicate lack of toxicity and apoptotic response. C) Phase I, II and III genes expressed specifically in the proximal tubule are strongly induced upon expression of Hnf1a and Hnf4a in combination. D)

Hnf1a and Hnf4a upregulate expression of epithelial markers Cdh1 and Tjp1. E) Slc22a6 exhibits function in transduced MEFs, as indicated by probenecid-sensitive uptake of organic anion 6-Carboxyfluorescein.

Table 1

## List of Drug-Metabolizing Enzymes and Transporters

PHASE I			
Gene Families		Additional Genes	
Symbol	Full Name	Symbol	Full Name
Adh	Alcohol dehydrogenase	Aadac	Arylacetamide deacetylase
Aldh	Aldehyde dehydrogenase	Cel	Carboxyl ester lipase
Aox	Alternative oxidase	Ddo	D-aspartate oxidase
Cbr	Carbonyl reductase	Dpyd	Dihydropyrimidine dehydrogenase
Ces	Carboxylesterase	Dpys	Dihydropyrimidinase
Cyb5	Cytochrome B5	Gsr	Glutathione reductase
Cyp	Cytochrome P450	Gusb	Glucuronidase
Dhrs	Dehydrogenase/Reductase (SDR Family) Member	Hagh	Hydroxyacylglutathione hydrolase
Ephx	Epoxide hydrolase	Hprt	Hypoxanthine guanine phosphoribosyl transferase
Fmo	Flavin-containing monooxygenase	Xdh	Xanthine dehydrogenase
Gpx	Glutathione peroxidase		
Hsd	Hydroxysteroid dehydrogenase		
Mao	Monoamine oxidase		
Pon	Paraoxonase		
Uchl	Ubiquitin carboxyl-terminal esterase		

PHASE II			
Gene Families		Additional Genes	
Symbol	Full Name	Symbol	Full Name
Acs	Acetyl-CoA synthetase	Aanat	Aralkylamine N-acetyltransferase
Agxt	Alanine-glyoxylate aminotransferase	As3mt	Arsenic (+3 oxidation state) methyltransferase
Akr	Aldo-keto reductase	Baat	Bile acid-CoA:amino acid N-acyltransferase
Alg	Asparagine-linked glycosylation	Ddost	Dolichyl-di-phosphooligosaccharide-protein glycotransferase
Ccbl	Cysteine conjugate-beta lyase	Faah	Fatty acid amide hydrolase
Chst	Carbohydrate sulfotransferase	Gamt	Guanidinoacetate N-methyltransferase
Comt	Catechol-O-methyltransferase	Glyat	Glycine-N-acyltransferase
Galnt	Polypeptide N-acetylgalactosaminyltransferase	Gnmt	Glycine N-methyltransferase
Gcnt	Glucosaminyl (N-acetyl) transferase	Hnmt	Histamine N-methyltransferase
Ggt	Gamma-glutamyltransferase	Inmt	Indolethylamine N-methyltransferase
Gst	Glutathione S-transferase	Nnmt	Nicotinamide N-methyltransferase
Mgat	Mannoside acetylglucosaminyltransferase	Pnmt	Phenylethanolamine N-methyltransferase
Mgst	Microsomal glutathione S-transferase	Tpmt	Thiopurine S-methyltransferase
Naa	N(alpha)-acetyltransferase		
Nat	N-acetyltransferase		
Nqo	NAD(P)H dehydrogenase		
Sat	Spermidine/spermine N1-acetyltransferase		
Sulf	Sulfatase		
Sult	Sulfotransferase		
Ugt	UDP-glycosyltransferase		

PHASE III			
Gene Families			
Symbol	Full Name		
Abcb	ATP-binding cassette transporter subfamily B (MDR/TAP)		
Abcc	ATP-binding cassette transporter subfamily C (MRP)		
Abcg	ATP-binding cassette transporter subfamily D (WHITE)		
Slc10	Solute Carrier Family 10 (sodium bile salt cotransport family)		
Slc15	Solute Carrier Family 15 (proton oligopeptide cotransporter family)		
Slc21	Solute Carrier Family 21 (organic anion transporter (SLCO) family)		
Slc22	Solute Carrier Family 22 (organic cation/anion/zwitterion transporter family)		
Slc47	Solute Carrier Family 47 (multidrug and Toxin Extrusion (MATE) family)		
Slc51	Solute Carrier Family 51 (transporters of steroid-derived molecules)		

**Note:** Drug transporters are sometimes also categorized as Phase 0 (influx) and Phase III (efflux). Here we use the more general classification of Phase III that includes all drug transporters.

**A**

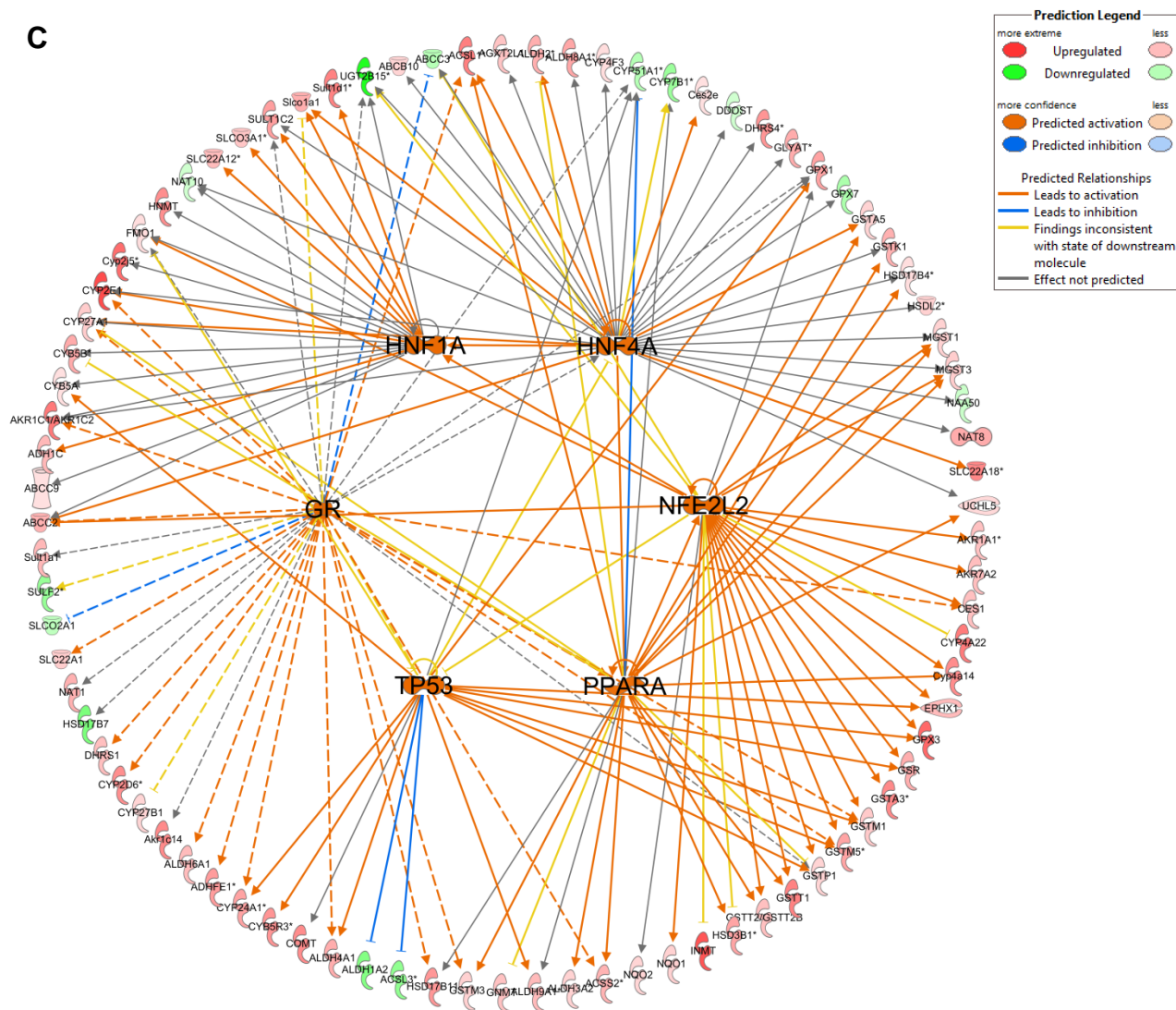
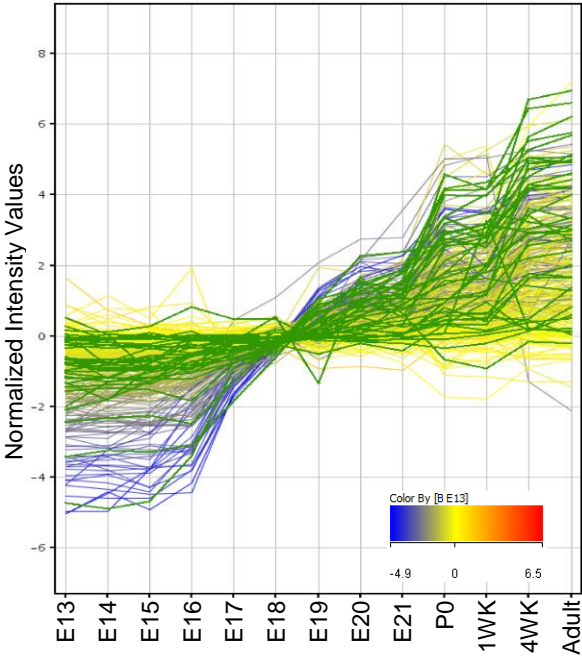
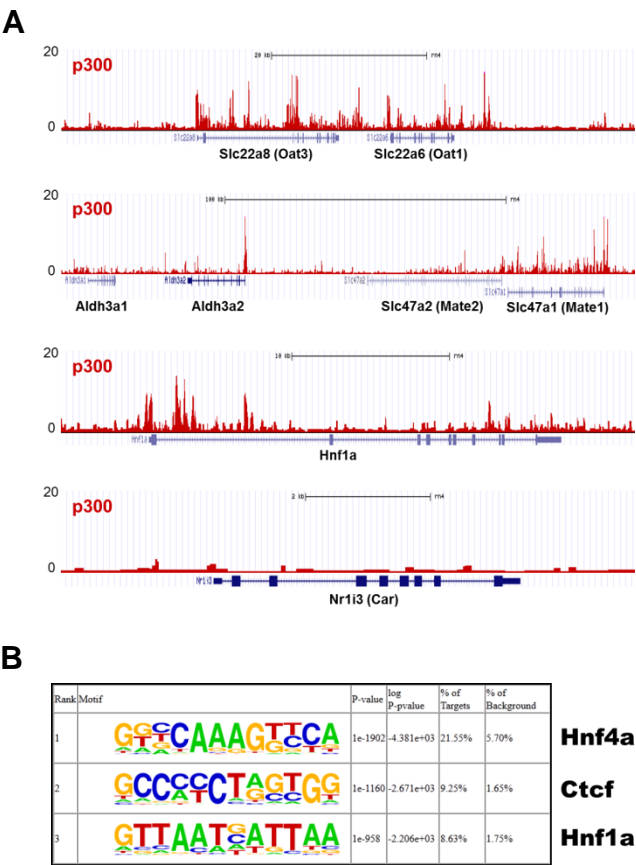
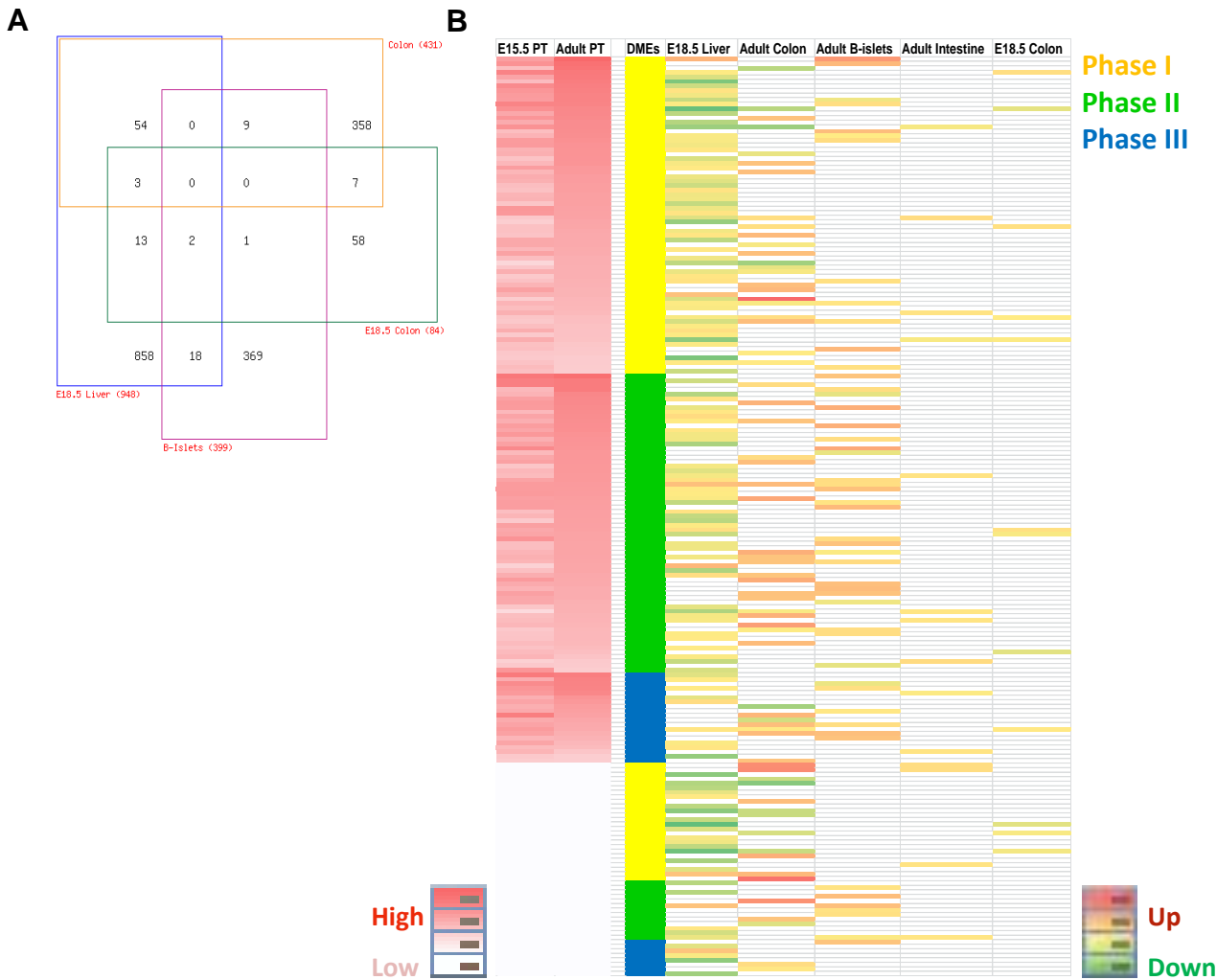


Figure 2







A

Sample	Unique ChIP Reads	Unique Input Reads	IP Efficiency	Peak Count
E20 Hnf4a	23,119,692	8,022,711	14.34%	38,145
P13 Hnf4a	18,343,314	8,070,141	22.34%	52,541
Adult Hnf4a	16,371,932	10,130,016	33.38%	79,871
Adult p300	11,726,046	7,785,098	18.04%	42,537

B

Peak Overlap (within 100bp)

	E20 Hnf4a	P13 Hnf4a	Adult Hnf4a	Cortex p300
E20 Hnf4a	38,145			
P13 Hnf4a	28,999	52,541		
Adult Hnf4a	30,205	44,981	79,871	
Cortex p300	14,966	20,209	25,171	42,537

Differential Peaks ( > 4-fold)

	E20 Hnf4a	P13 Hnf4a	Adult Hnf4a
E20 Hnf4a		13,432	46,325
P13 Hnf4a	6,285		17,706
Adult Hnf4a	6,221	1,856	



